



TechnoChem

International Journal of TechnoChem Research

ISSN:2395-4248

www.technochemsai.com

Vol.03, No.03, pp 281-291, 2017

Modeling and Simulation of SRF and PI Controlled Dstatcom for Power Qualirt Enhancement

Prasad Miska¹, Ashok Kumar Akella²

¹⁻²Department of Electrical Engineering, National Institute of Technology Jamshedpur, Jharkhand 831014, India

Abstract: This paper describes the comparative analysis of the steady state behavior of two different control techniques of distributed flexible AC transmission system (DFACTS) controller called as distributed static synchronous compensator (DSTATCOM), aimed at power quality (PQ) enhancement in terms of voltage swell mitigation in a three-phase four-wire (3p4w) distribution system. A DSTATCOM is one of the major power quality improvement devices which consist of a DC energy source, a voltage source inverter (VSI), a filter, a coupling transformer and the control system. The control strategy based on synchronous reference frame (SRF) theory and propositional-integral (PI) controller has been used for reference current generation of voltage source inverter (VSI) based DSTATCOM. The SRF and PI control based DSTATCOM is validated through dynamic simulation in a MATLAB\SIMULINK environment under linear as well as nonlinear loads.

Keywords- Power quality, Voltage swell, DSTATCOM, SRF, PI, VSI

1. Introduction

Recent work on worldwide power distribution shows a substantial growing number of sensitive loads such as hospital equipment, industry automations, semiconductor device manufacturer. The most common characteristics of these loads in modern industry and commercial applications are their ability to produce voltage sags and swells. According to an EPRI report, the economic losses due to poor power quality are \$400 billion, a year in the U.S alone^{1,2}. According to IEEE standard a voltage swell is defined as an increase in root mean square voltage from 110% to 180% of the normal voltage at the power frequency for the duration from 0.5 cycles of 1 minute. A voltage swell can occur due to a fault switching off a large load and switching to a large capacitor bank^{3,4}. Voltage Swells are characterized by their magnitude and duration⁵. There, are many different solutions have been proposed to eliminate voltage swells⁶, conventionally the passive filters are used for power quality issues. But nowadays power electronics based on new kind of emerging custom power devices such as Dynamic voltage restorer, Distributed static compensator and unified power quality conditioner have been more popular because they offer the advantages of flexibility and high performance to improve the controllability of power distribution network⁷. The DSTATCOM is one of the solid state shunt connected CPD, which is one of the victorious solution to enhance different significant aspects of power quality⁸⁻¹¹. Performance of DSTATCOM depends upon the control algorithm used for reference current calculation and firing pulse generation strategy. Most common and popularly used control strategies for 3p4w DSTATCOM are an instantaneous active power theory, symmetrical component theory, improved instantaneous active and reactive current component theory¹², p-q and p-q-r theory¹³, hysteresis current controller technique¹⁴, d-q reference frame or synchronous reference frame theory¹⁵, etc. In this work, synchronous reference frame theory and propositional-integral controller are used for the control of VSI based DSTATCOM. A new configuration of DSTATCOM is proposed for a three-phase four-wire power distribution system, which is based on six-leg VSI. The DSTATCOM is modulated and simulated using time-domain MATLAB\Simulink platform to mitigate

voltage swell under linear and nonlinear load. Comparative analysis of the control strategies under linear and nonlinear loads in between without compensator and with compensator is presented.

2. Description of Dstatcom Configuration

Figure 1 shows a schematic diagram of a shunt connected power electronic based DSTATCOM with balance resistive-capacitive (R-C) and diode-rectifier load connected to a three-phase four-wire distribution network having a source resistance and inductance. The DSTATCOM produces suitable compensating currents (i_{Ca}, i_{Cb}, i_{Cc}) and injected to each phase of the system to eliminate voltage swells. To filter high-frequency components of compensating currents, an interfacing inductance L_f is used at AC side of the voltage source inverter based DSTATCOM.

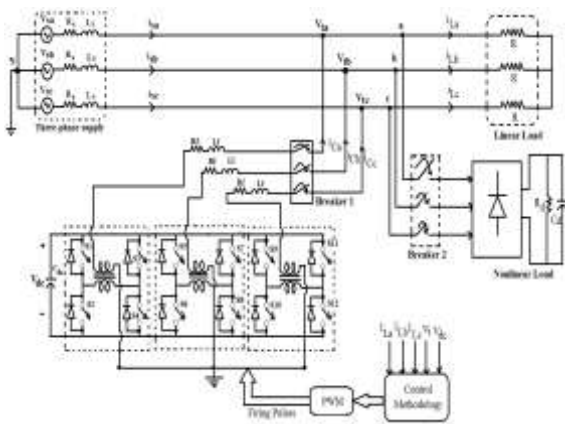


Fig.1. Schematic diagram of VSI-based DSTATCOM

3. Mathematical Modeling of Distrubution System

This part shows the mathematical modeling of the supply system, shunt connected DSTATCOM and nonlinear load.

3.1 Mathematical Modeling of Supply System

The supply system modeling can be represented in terms of volt-ampere equations as:

$$V_{Sa} = i_{Sa} R_{Sa} + V_{La} + V_{ta} \quad (1)$$

Where $V_{La} = L_{Sa} \left(\frac{di_{Sa}}{dt} \right)$ then the equation (1) can be rewritten as

$$V_{Sa} = i_{Sa} R_{Sa} + L_{Sa} \left(\frac{di_{Sa}}{dt} \right) + V_{ta} \quad (2)$$

$$V_{Sb} = i_{Sb} R_{Sb} + L_{Sb} \left(\frac{di_{Sb}}{dt} \right) + V_{tb} \quad (3)$$

$$V_{Sc} = i_{Sc} R_{Sc} + L_{Sc} \left(\frac{di_{Sc}}{dt} \right) + V_{tc} \quad (4)$$

Where, V_{Sa} , V_{Sb} and V_{Sc} are the three-phase supply voltages, i_{Sa} , i_{Sb} and i_{Sc} are the three-phase supply currents, V_{ta} , V_{tb} and V_{tc} are the three-phase terminal voltages at the point of common coupling (PCC), R_G and

L_S are the supply resistance and inductance of the supply respectively. Equation (2) (3) and (4) can be rewritten in the form of state space derivative as:

$$\frac{di_{Sa}}{dt} = \frac{(V_{Sa} - V_{ta} - i_{Sa}R_{Sa})}{L_{Sa}} \quad (5)$$

$$\frac{di_{Sb}}{dt} = \frac{(V_{Sb} - V_{tb} - i_{Sb}R_{Sb})}{L_{Sb}} \quad (6)$$

$$\frac{di_{Sc}}{dt} = \frac{(V_{Sc} - V_{tc} - i_{Sc}R_{Sc})}{L_{Sc}} \quad (7)$$

3.2 Modeling of Voltage Source Inverter-Based Dstatcom

$$V_{ta} = i_{Ca}R_c + L_c \left(\frac{di_{Ca}}{dt} \right) + v_{Ca} \quad (8)$$

$$V_{tb} = i_{Cb}R_c + L_c \left(\frac{di_{Cb}}{dt} \right) + v_{Cb} \quad (9)$$

$$V_{tc} = i_{Cc}R_c + L_c \left(\frac{di_{Cc}}{dt} \right) + v_{Cc} \quad (10)$$

$$V_{Nc} = -i_{Nc}R_c - L_c \left(\frac{di_{Nc}}{dt} \right) \quad (11)$$

Where, i_{Ca} , i_{Cb} and i_{Cc} are the three-phase DSTATCOM currents, v_{Ca} , v_{Cb} and v_{Cc} are the three-phase DSTATCOM AC voltages, V_{Nc} is the DSTATCOM neutral voltage, R_c and L_c are DSTATCOM resistance and inductance respectively. The first order differential equations for the derivatives of DSTATCOM currents can be represented in the form of state space equations:

$$\frac{di_{Ca}}{dt} = \frac{(V_{ta} - v_{Ca} - i_{Ca}R_c)}{L_c} \quad (12)$$

$$\frac{di_{Cb}}{dt} = \frac{(V_{tb} - v_{Cb} - i_{Cb}R_c)}{L_c} \quad (13)$$

$$\frac{di_{Cc}}{dt} = \frac{(V_{tc} - v_{Cc} - i_{Cc}R_c)}{L_c} \quad (14)$$

3.3 Modeling of Nonlinear Load

The three-phase diode-rectifier with capacitive-resistive (R-C) load is considered as nonlinear load. The basic equations for the three-phase non-linear loads are represented as:

$$V_{Sa} = V_{La} + i_{La}R_{sa} + L_{Sa} \left(\frac{di_{La}}{dt} \right) \quad (15)$$

$$V_{Sb} = V_{Lb} + i_{Lb} R_{sb} + L_{Sb} \left(\frac{di_{La}}{dt} \right) \quad (16)$$

$$V_{Sc} = V_{Lc} + i_{Lc} R_{sc} + L_{Sc} \left(\frac{di_{Lc}}{dt} \right) \quad (17)$$

Where V_{La} , V_{Lb} and V_{Lc} are load voltages across load capacitors. The state space equations for three phase nonlinear load can be written as:

$$\left(\frac{di_{La}}{dt} \right) = \frac{(V_{Sa} - V_{La} - i_{La} R_{sa})}{L_{Sa}} \quad (18)$$

$$\left(\frac{di_{Lb}}{dt} \right) = \frac{(V_{Sb} - V_{Lb} - i_{Lb} R_{sb})}{L_{Sb}} \quad (19)$$

$$\left(\frac{di_{Lc}}{dt} \right) = \frac{(V_{Sc} - V_{Lc} - i_{Lc} R_{sc})}{L_{Sc}} \quad (20)$$

4. Dstatcom Control Strategies

Control strategy plays the most important role in any custom power devices (CPDs). The performance of a D-STATCOM system solely depends upon its control technique for generation of reference signals (current and voltage). For this purpose, there is several control algorithms are presented in literature, and some commonly used control techniques are Synchronous Reference Frame (SRF) theory¹⁶, Sinusoidal Pulse Width Modulation (SPWM) technique¹⁷, Adaptive Neuro Fuzzy interface system (ANFIS) technique¹⁸, Instantaneous Active and Reactive Current (IARC) theory and PID control technique¹⁹. Among these control approaches, SRF and PI control techniques are popularly used.

4.1 Synchronous Reference Frame (SRF) Theory

This control scheme is based on the transformation of load currents (i_{La}, i_{Lb}, i_{Lc}) from a-b-c frame to the synchronously rotating reference frame to extract the direct, quadraure and zero-sequence components. A block diagram of the control topology is shown in Figure 2.

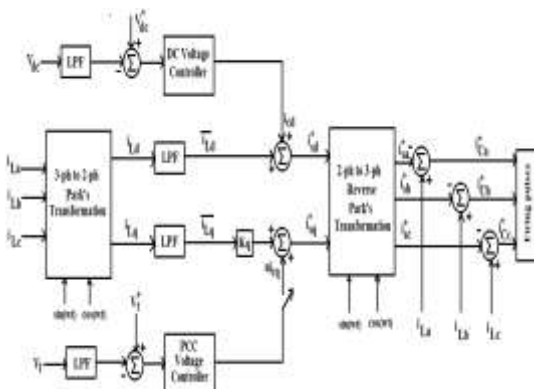


Fig. 2. Block diagram of SRF controller

$$\begin{bmatrix} i_{Ld} \\ i_{Lq} \\ i_{Lo} \end{bmatrix} = (2/3) \begin{bmatrix} \cos \theta & -\sin \theta & 0.5 \\ \cos(\theta - 120^\circ) & -\sin(\theta - 120^\circ) & 0.5 \\ \cos(\theta + 120^\circ) & -\sin(\theta + 120^\circ) & 0.5 \end{bmatrix} \begin{bmatrix} i_{La} \\ i_{Lb} \\ i_{Lc} \end{bmatrix} \quad (21) \quad i_{sd}^* = \overline{i_{Ld}} + i_{Cd}$$

$$i_{sq}^* = K_q \overline{i_{Lq}} + u i_{Cq} \quad (23)$$

Where, $\overline{i_{Ld}}$ and $\overline{i_{Lq}}$ are the average values of the d- axis and q-axis components of the load currents.

$$\begin{bmatrix} \overline{i_{Ld}} \\ \overline{i_{Lq}} \end{bmatrix} = G(s) \begin{bmatrix} i_{Ld} \\ i_{Lq} \end{bmatrix} \quad (24)$$

Where $G(s)$ is the transfer function and logical variable, $u = 0$ if the power factor is to be regulated and $u = 1$ if bus voltage is to be regulated. $K_q=1$ in the latter case.

$$K_q = \frac{Q_L^*}{Q_L} \quad (25)$$

The reference for the source current is the d-q frame and first converted to the α - β frame and then to the a-b-c frame using following formulation.

$$\begin{bmatrix} i_{s\alpha}^* \\ i_{s\beta}^* \end{bmatrix} = \begin{bmatrix} \cos(\omega t) & \sin(\omega t) \\ -\sin(\omega t) & \cos(\omega t) \end{bmatrix} \begin{bmatrix} i_{sd}^* \\ i_{sq}^* \end{bmatrix} \quad (26)$$

$$\begin{bmatrix} i_{sa}^* \\ i_{sb}^* \\ i_{sc}^* \end{bmatrix} = \sqrt{\frac{2}{3}} \begin{bmatrix} 1 & 0 \\ -1/2 & -\sqrt{3}/2 \\ -1/2 & \sqrt{3}/2 \end{bmatrix} \begin{bmatrix} i_{sa}^* \\ i_{sb}^* \end{bmatrix} \quad (27)$$

Hence

$$\begin{bmatrix} i_{sa}^* \\ i_{sb}^* \\ i_{sc}^* \end{bmatrix} = \sqrt{\frac{2}{3}} \begin{bmatrix} \cos(\omega t) & \sin(\omega t) \\ \cos(\omega t - (2\pi/3)) & \sin(\omega t - (2\pi/3)) \\ \cos(\omega t + (2\pi/3)) & \sin(\omega t + (2\pi/3)) \end{bmatrix} \begin{bmatrix} i_{sd}^* \\ i_{sq}^* \end{bmatrix} \quad (28)$$

The reference for the source current vectors ($i_{sa}^*, i_{sb}^*, i_{sc}^*$) are compared and the desired compensator currents ($i_{Ca}^*, i_{Cb}^*, i_{Cc}^*$) are obtained as the difference between the load and the source currents.

$$\begin{cases} i_{Ca}^* = i_{La} - i_{sa}^* \\ i_{Cb}^* = i_{Lb} - i_{sb}^* \\ i_{Cc}^* = i_{Lc} - i_{sc}^* \end{cases} \quad (29)$$

4.2 Proportional–Integral (PI) Controller

Block diagram of PI controller is depicted in Figure 3. Three-phase source voltage (V_{abc_s}) is continuously measured the control system and is compared with a reference voltage (V_{ref}) and generates a voltage error (V_{error}) signal. This error signal is given to the PI controller as an input, the PI controller process this error signal and produces an angle δ to drive the error to zero. From the phase-shift angle δ , the three-phase sinusoidal signal $V_{control}$ is obtained as:

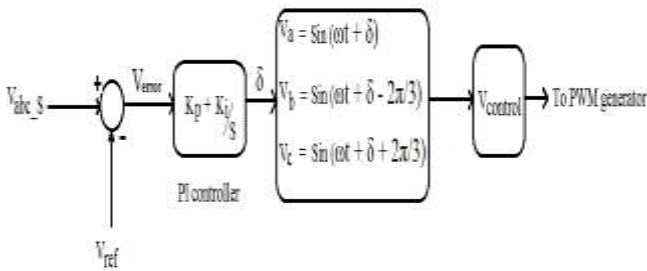


Fig.3. PI Controller

$$\left. \begin{aligned}
 V_a &= \text{Sin}(\omega t + \delta) \\
 V_{\text{Control}} = V_b &= \text{Sin}\left(\omega t + \delta - \frac{2\pi}{3}\right) \\
 V_c &= \text{Sin}\left(\omega t + \delta + \frac{2\pi}{3}\right)
 \end{aligned} \right\} \quad (30)$$

In PWM generator, sinusoidal signal is compared with a carrier signal and generates triggering pulses. This triggering or firing pulses are given to the gate terminal of the insulated gate bipolar transistor (IGBT) switches to switch on the VSI based DSTATCOM under voltage swell condition.

5. Simulation of Dstatcom

Figure 1 shows the proposed configuration of the test system used to carry out the transient modeling and simulation of the DSTATCOM with associated control strategy. This DSTATCOM model is simulated with the SRF and PI control techniques with simulation period 0.3s. The electrical power system parameters are summarized in Table 1.

Table 1. Network parameters used in the Simulink

Parameter	Value
Source voltage	$V_s = 415 \text{ V}, 50 \text{ Hz}$
Line impedance	$Z_s = 1.57 + j15.70 \ \Omega$
Linear load	$P = 40 \text{ W}, Q = 20 \text{ VAR}$
Nonlinear load	Diode-Rectifier with $R_d = 400 \ \Omega, L_d = 50 \text{ mH}$
Filter parameter	$L_f = 7.0 \ \mu\text{F}$
DC side voltage and capacitance	$V_{dc} = 7000 \text{ V}, C_{dc} = 2000 \ \mu\text{F}$
Proportional and PI controller	$K_{pi} = 0.6, k_{p2} = -0.2, k_i = -40$

6. Simulation Results and Discussion

In this section, simulation results of two control topologies used in three-phase four-wire DSTATCOM supplying two loads are presented. Load1 is considered as fixed resistive load (R-load) and load2 is considered as variable linear and nonlinear load. The variable linear load is taken as three-phase resistive-capacitive (R-C) whereas nonlinear load is realized by three-phase diode-rectifier with R-C load. Breaker 1 is used to control the period of operation of VSI-based DSTATCOM and breaker 2 is used to control the connection of variable load to the distribution network. Initially, both the loads are connected to the network, but after a certain period of time load2 are switched off by opening the breaker2. Due to sudden removal of heavy load, voltage swell occurs in the source voltage. The objective of the simulation is to study two different performance aspects for voltage source inverter based DSTATCOM: 1) Voltage swell mitigation, by SRF control based DSTATCOM under linear and nonlinear load and 2) Voltage swell mitigation, by PI control based DSTATCOM under linear and nonlinear load.

6.1 Voltage Swells Mitigation by SRF Control Based Dstatcom under Linear Load

Due to switching off a three-phase linear load by opening breaker2, a three-phase balanced voltage swell occurs in the source terminal of the distribution network from 0.1 to 0.25s. Then the voltage signal recovers to its normal value. During three-phase balanced voltage swell, voltage magnitude of all the three phases may reach a level of 205% as shown in Figure 4(a). For balanced voltage swell of 65%, the source voltage signal before compensation, the compensation current, the load voltage after voltage swell compensation are depicted in Figure 4 (a) to (c). As figure shows, the proposed SRF control based voltage swell compensator restore the voltage on the load side by injecting proper compensating current in each phase so that the load voltage remains at the desired level. The performance of SRF control based uncompensated and compensated load voltages under linear load are shown in Figure 5. As the figure shows when the compensator is connected, the voltage at the load terminal reaches rapidly to the normal levels 140V. This can be resolved by injecting the appropriate amount of current to the distribution network under voltage swell conditions

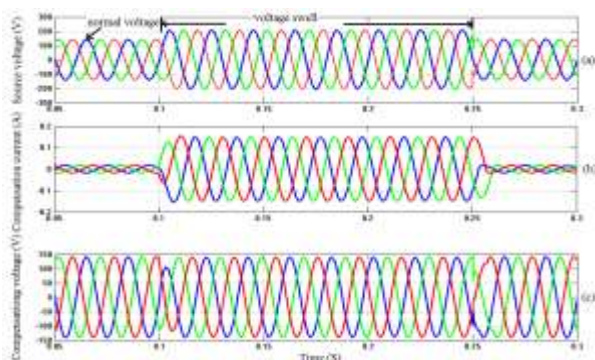


Fig. 4. Voltage swells under linear load with SRF controller

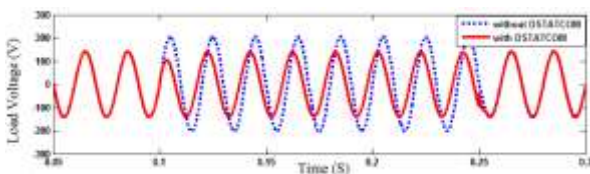


Fig. 5. Load voltage with and without DSTATCOM by SRF controller

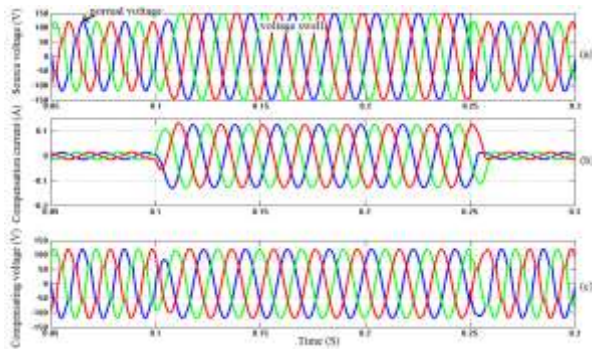


Fig. 6. Voltage swell under nonlinear load with SRF theory

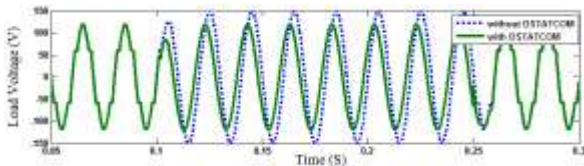


Fig. 7. Load voltage with and without DSTATCOM by SRF controller.

6.2 Voltage Swells Mitigation by SRF Method under Nonlinear Load

Figure 6 (a) to (c) depicts the simulation results of SRF control based DSTATCOM with nonlinear load. In this case the three-phase source voltage magnitude raised to 30% of the normal level for the duration of 0.24 s. Then voltage recovers to its normal level. As it can be observed from the simulation results, the SRF control based DSTATCOM is able to generate the desired current components for three-phases rapidly and helps to maintain load voltage sinusoidal at the normal value. Figure 7 depicts the load voltages under nonlinear load conditions with and without voltage swell compensator. As the graph shows when SRF control based voltage swell compensator is added to the distribution system, it produces required amount of compensation current in each phase rapidly, so that the load voltage remains at the acceptable level.

6.3 Voltage Swells Mitigation by PI Controller under Linear Load

Figure 8 (a) to (c) shows the simulation results of PI controller based DSTATCOM with linear load. In this case voltage swell of 40% has happened in all the three-phases, which starts at $t=0.10$ s and ends at $t=0.25$ s. From the figure 15 (b) and (c) it is observed that PI controller based DSTATCOM is able to produce the required current components for three-phases and helps to maintain load voltage sinusoidal at the normal level. Figure 9 shows the load voltages under linear load with and without voltage swell compensator. As it can be seen, after the voltage swell compensator connected, voltage swell disappears and load voltage recovers their normal value (245V).

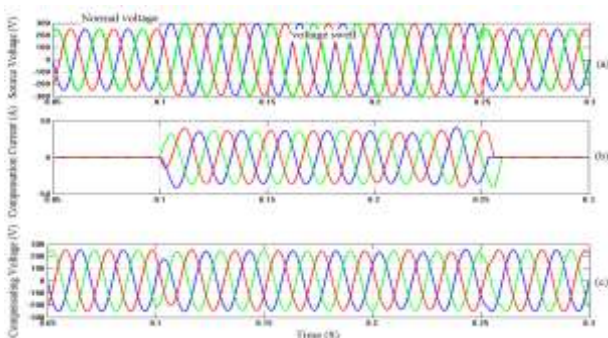


Fig.8 Voltage swells under linear load with PI control scheme

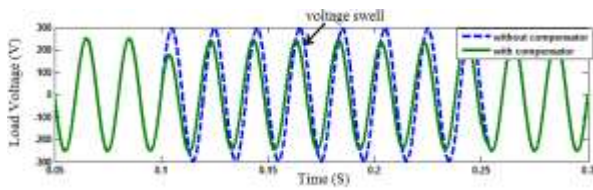


Fig.9.Load voltage with and without compensator under linear load with PI controller

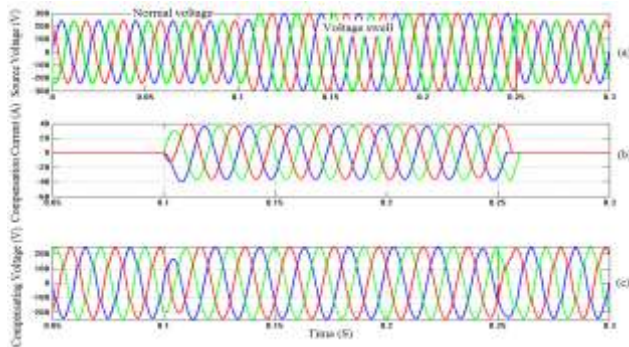


Fig.10 Voltage swells under nonlinear load with PI control scheme

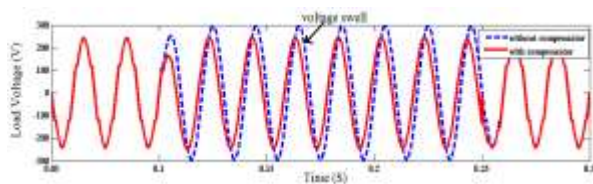


Fig.11.Load voltage with and without compensator under nonlinear load with PI controller

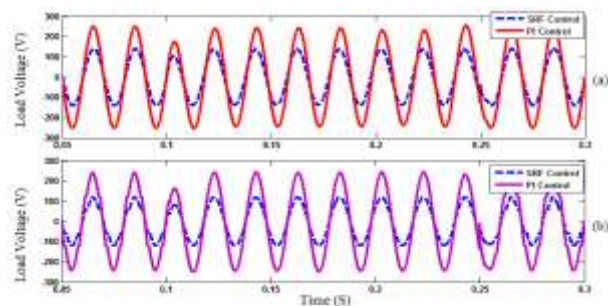


Fig.12.Comparison of load voltage under SRF and PI control techniques (a) linear load and (b) Nonlinear

6.4 Voltage Swells Mitigation by PI Controller under Nonlinear Load

Figure A three-phase balanced voltage swell of magnitude 52% occurs in the source terminal of the system from 0.10 to 0.25s. During three-phase balanced voltage swell, the voltage magnitude of all the three-phases may reach a level of 295% as shown in Figure 10 (a). For balanced voltage swell of 52%, the source voltage signal before compensation, the compensation current, the load voltage after voltage swell compensation are depicted in Figure 10 (a) to (c). As figure shows, the proposed PI control based DSTATCOM restore the voltage on the load side immediately by injecting required amount of compensating current in each phase so that the load voltage remains at the acceptable level. Compensated and uncompensated load voltages under nonlinear load are depicted in Figure 11. As the graph shows when the voltage swell compensator is connected, the voltage at the load terminal reaches rapidly to the normal levels 245V. Figures 12(a) and (b) show the performance comparison of SRF and PI control based DSTATCOM for voltage swell mitigation under linear as well as nonlinear loads. SRF and PI control based voltage swell compensator mitigate the voltage swell of magnitude 65% and 40% under linear load and 30% and 52% under nonlinear load condition.

7. Analysis of Simulation Results

Comparative evaluation of two different control schemes is shown in Table 2. It can be noted from Table 2 that PI control method is simple with respect to computational complexity because it does not require any transformation (Parks and Clarks). PI control based DSTATCOM mitigate the voltage swell of magnitude 40% and 52% under linear as well as nonlinear load conditions. On the other hand SRF control based DSTATCOM mitigate voltage swell of magnitude 65% and 30%.

Table 2. Comparison of SRF and PI control strategies

Parameters	Various Control Techniques	
	SRF Controller	PI Controller
Computational complexity	It requires complex transformation	It does not require complex transformation
Phase locked loop (PLL)	It requires phase locked loop	It does not require phase locked loop
Voltage Swell mitigation	Excellent	Good

8. Conclusion

In this work, a comparative analysis of two different control schemes for DSTATCOM installed in three-phase four wire distribution systems has been presented. The performance of these control techniques has been analyzed for voltage swell mitigation using time-domain MATLAB/Simulink software under three-phase linear and nonlinear load conditions. In contrast, SRF theory needs additional PLL circuit for calculation of angle ' θ ' whereas in PI control method angle ' θ ' is directly calculated from main voltages. PI controller is simple as it does not require Clarks or Parks transformation. The obtained simulation results from both control schemes are excellent or even slightly better in SRF control in compared with PI control.

References

1. Sadigh, A.K., Smedley, K.M., Fast and precise voltage sag detection method for dynamic voltage restorer (DVR) application, *Electric Power Systems Research*, 2016, 130; 192–207.
2. Latran, M.B., Teke, A., Yoldas, T., Mitigation of power quality problems using distributed static synchronous compensator: a comprehensive review, *IET Power Electronics*, 2015, 8; 1312-1328.
3. Venkatesh, C., Siva Sarma, D.V.S.S., Sydulu M., Mitigation of Voltage Sag/Swell Using Peak Detector Based Pulse Width Modulation Switched Autotransformer. *Electric Power Components and Systems*, 2011, 39; 1117–1133.
4. Fuchs, E.F., Masoum, M.A.S; *Power quality in power systems and electrical machines*. Perth, WA, Australia, 2008.
5. Alam, M.R, Muttaqi, K.M., Bouzardoum, A; Characterizing voltage sags and swells using three-phase voltage Ellipse parameters, *IEEE Transaction on Industry Application*, 2015, 51; 2780-2790.
6. Babaei, E., Nazarloo, A., Hosseini, S.H; Application of Flexible Control Methods for DSTATCOM in Mitigating Voltage Sags and Swells, *IPEC Conference*, 2010, 590-595.
7. Singh, A; Performance Evaluation of Three Different Configurations of DSTATCOM with Nonlinear Loads, *IETE Journal of Research*, 2010, 56; 313-326.
8. Sundarabalan, C.K., Selvi, K., Compensation of voltage disturbances using PEMFC supported Dynamic Voltage Restorer. *Electrical Power and Energy Systems*, 2015, 71; 77-92.
9. Eskander, M.N., Amer, S.I., Mitigation of Voltage Dips and Swells in Grid-connected Wind Energy Conversion Systems, *IETE Journal of Research*, 2011, 57; 515-524.
10. Rahman, S.A., Janakiraman, P.A., Somasundaram, P., Voltage sag and swell mitigation based on modulated carrier PWM. *Electrical Power and Energy Systems*, 2015, 66; 78–85.

11. Zaveri, T., Bhalja, B., Zaveri, N., Comparison of control strategies for DSTATCOM in three-phase, four-wire distribution system for power quality improvement under various source voltage and load conditions. *Electrical Power and Energy Systems*, 2012, 43;582-594.
12. Aredes, M., Akagi, H., Watanabe, E.H., et al., Comparisons Between the p-q and p-q-r Theories in Three-Phase Four-Wire Systems, *IEEE Transactions on Power Electronics*, 2009, 24;924-933.
13. Gupta, R., Generalized Frequency Domain Formulation of the Switching Frequency for Hysteresis Current Controlled VSI Used for Load Compensation, *IEEE Transactions on Power Electronics*, 2012, 27, 2526-2535.
14. Da silva, CH., Pereira, R.R., da silva LEB, et al., *A digital PLL scheme for three-phase system using modified synchronous reference frame*, *IEEE Transactions Industrial Electronics*, 2010, 57;3814-21.
15. Li, S., Xu, L., Haskew, T.A., Control of VSC-based STATCOM using conventional and direct-current vector control strategies. *Electrical Power and Energy Systems*, 2013, 45; 175-186.
16. Georgios, K., Georgios, T., Georgios, A., A multifunction control scheme for current harmonic elimination and voltage sag mitigation using a three phase three level flying capacitor inverter, *Simulation Modelling Practice and Theory*, 2012, 24;15-34.
17. Balikci, A., Akpınar, E.; A multilevel converter with reduced number of switches in STATCOM for load balancing. *Electric Power Systems Research*, 2015, 123;164-173.
18. Rao, G.N., Raju, P.S., Sekhar, K.C., Harmonic elimination of cascaded H-bridge multilevel inverter based active power filter controlled by intelligent techniques. *Electrical Power and Energy Systems*, 2014, 61;56-63.
19. Jing, X., Cheng, L., An optimal PID control algorithm for training fed-forward neural networks, *IEEE Transaction Industrial Electronics*, 2013, 60;2273-228.
